

Targeting the genome stability hub Ctf4 by stapled-peptide design

Yuteng Wu^{b*}, Fabrizio Villa^{c*}, Joseph Maman^{a*}, Yu H Lau^b, Lina Dobnikar^b, Aline Simon^a, Karim Labib^c,
David R Spring^b, Luca Pellegrini^a

^a Department of Biochemistry, University of Cambridge, Sanger Building, 80 Tennis Court Road,
Cambridge CB2 1GA, United Kingdom

^b Department of Chemistry, University of Cambridge, Lensfield Road, Cambridge CB2 1EW, United
Kingdom

^c School of Life Sciences, University of Dundee, Dow Street, Dundee DD1 5EH, United Kingdom

* These authors contributed equally to this manuscript.

For correspondence: Karim Labib (kpmlabib@dundee.ac.uk), David Spring (spring@ch.cam.ac.uk),
Luca Pellegrini (lp212@cam.ac.uk)

Exploitation of synthetic lethality by small-molecule targeting of molecular pathways that maintain genomic stability has attracted much interest as a chemotherapeutic tool. The Ctf4/AND-1 protein factor, an evolutionarily conserved hub that links DNA replication, DNA repair and chromosome segregation, represents in principle an attractive target for the synthetic lethality approach. The recent elucidation of the recruitment mechanism to yeast Ctf4 of its protein partners has provided a structural basis for proof-of-principle development of molecular agents that interfere with its hub function. Here we report the design, optimization, biochemical and structural validation of double-click stapled peptides encoding the Ctf4-interacting peptide (CIP) motif of the replicative helicase subunit GINS Sld5. By screening stapling positions in the Sld5 CIP sequence, we identified an unorthodox *i,i+6* stapled peptide with improved, sub-micromolar binding to Ctf4 relative to the wild-type CIP. The mode of interaction with Ctf4 was confirmed by a crystal structure of the stapled Sld5 peptide bound to the C-terminal domain of Ctf4 (Ctf4_{CTD}). The stapled Sld5 peptide was able to displace the Ctf4-partner DNA polymerase α from the replisome in yeast extracts. These findings provide experimental evidence in support of development of small-molecule inhibitors of the human-CTF4 orthologue AND-1.

Introduction

Targeting cancer cells with DNA-damaging agents such as cis-platin is a mainstay of traditional chemotherapy, and its effectiveness might reflect the underlying fragility of cancer cells in maintaining their genomic stability¹. More recently, the concept of synthetic lethality as the Achilles heel of cancer cells with defective pathways of genome stability maintenance has taken firm hold, since the pioneering observations that breast cancer susceptibility protein 2 (BRCA2)-null cancer cells are exquisitely sensitive to inhibitors of poly(ADP-ribose) polymerase (PARP)^{2,3}. Alongside DNA-damaging agents, small-molecule inhibitors of proteins with essential roles in DNA synthesis, such as the DNA polymerase inhibitor fludarabine^{4,5} and topoisomerase inhibitors camptothecin and etoposide^{6,7}, are currently used in clinical practice. As DNA replication and repair processes cooperate to preserve genomic integrity, synthetic lethality effects might exist, and should be searched for, among all chromosome instability (CIN) genes.

A distinctive feature of metabolic processes such as DNA replication, repair and transcription is the high degree of conservation of their protein components among eukaryotes. This observation has recently been exploited to screen CIN genes in yeast, as a quick way of identifying potentially druggable candidates displaying synthetic lethality with DNA repair genes that are often mutated in human cancers^{8,9}. Such analysis highlighted Ctf4 (Chromosome Transmission Fidelity 4)^{10,11} as a highly promising candidate, at a centre of a web of negative genetic interactions with other CIN genes. Moreover, the same appears to be true for the human orthologue of yeast Ctf4,¹². The high level of genetic connections involving Ctf4 is likely to reflect its known role as a protein hub linking different processes pertaining to chromosome stability, such as DNA replication and sister chromatid cohesion^{13,14} (Figure 1).

Ctf4 does not possess intrinsic enzymatic activity and therefore lacks an active site, making it harder to target with traditional small-molecule screening strategies. Our recent work has elucidated a key mechanism of recruitment to Ctf4 of its protein partners: binding is mediated by a short linear motif (SLIM)^{15,16}, known as the Ctf4-interacting peptide (CIP), which docks in α -helical form onto an exposed site on the helical domain of Ctf4, fused to Ctf4's second β -propeller domain (Figure 1)^{13,14}. The interaction is of moderate, micromolar affinity and represents an example of the SLIM-protein interactions that characterise the dynamic architecture of the replisome¹⁷. The determination of the structural basis for the interaction of Ctf4 with its client proteins has afforded an opportunity to develop a strategy for targeting Ctf4, by interfering with its function as a protein hub.

Targeting protein-protein interfaces (PPIs) as a means of specifically disrupting the association between macromolecules would increase greatly the range of druggable protein targets, and a lot of effort has gone into developing effective PPI inhibitors¹⁸⁻²⁰. Traditional small molecule library approaches are often not suitable for inhibiting PPIs though, as such interfaces consist usually of large and relatively flat surfaces. A promising approach to generate α -helical PPI inhibitors is the use of conformationally-constrained peptides, often referred to as 'stapled peptides', especially when referring to a peptide constrained into an α -helical conformation²¹⁻²³. In addition to their potential value as inhibitors, stapled peptides represent useful proof-of-principle tools to identify targetable interactions of interesting proteins with their physiological partners, and to dissect biological pathways.

Peptide stapling is a macrocyclisation approach in which helical peptides are covalently modified by the formation of a chemical linkage (staple) between side chains of two amino acids²⁴. The residues to be linked together are usually located on the same face of the peptide helix, and separated by one, two or three helical turns, so that one amino acid at position i is linked to position $i+4$, $i+7$ or $i+11$, respectively. Stapling can constrain α -helical peptides into their bioactive conformation, improving target affinity and overall pharmacokinetics²⁵. When optimised, peptide stapling can generate potent *in vivo* inhibitors of intracellular PPI targets²⁶⁻²⁸. We have recently pioneered a two component double-click stapling technique that makes use of double Cu(I)-catalysed azide-alkyne cycloaddition (CuAAC) between diazido peptides with dialkynyl staple linkages^{29,30}. This approach enables a range of different stapled peptides to be efficiently generated by reacting a single linear diazido peptide with a collection of different dialkynyl stapling linkages (Figure 2A).

In this paper, we describe the design of a stapled peptide targeting the interaction of Ctf4 with its client proteins (Figure 2B), based on the CIP sequence present in the GINS Sld5 subunit of the replicative helicase complex Cdc45-MCM-GINS (CMG)¹³. The most-effective stapled peptide bound to Ctf4 in the same fashion as the wild-type sequence, as determined by X-ray crystallography of the Sld5 CIP bound to Ctf4 C-terminal domain (Ctf4_{CTD}), but with about 10-fold increased affinity. Interestingly, the α -helix of the stapled peptide was conformationally constrained by an unorthodox $i,i+6$ spacing; to the best of our knowledge, this is the first time that the $i,i+6$ constraint has been used to improve helical content and target binding. Furthermore, the stapled CIP was able to disrupt the biochemical interaction between Ctf4_{CTD} and GINS *in vitro* and to detach the Ctf4-client DNA polymerase α from the replisome in yeast extracts. Our study provides the first proof-of-principle evidence that it is possible to develop chemical tools to target the Ctf4 hub in the eukaryotic replisome.

RESULTS

Rationale for chemical synthesis of stapled peptides

We had previously found that the GINS subunit Sld5 is responsible for anchoring Ctf4 to the CMG helicase, and showed that binding is mediated by the interaction of a short sequence motif of Sld5 (Ctf4-interacting peptide or CIP; 1-MDINIDDILAELDKETTAV-19) with an exposed site in the helical domain of the Ctf4_{CTD} structure¹³ (Figure 3A). Alanine-scanning mutagenesis had revealed that the hydrophobic amino acids I5, I8 and L9 at the binding interface were critical for interaction with Ctf4¹³. Keeping the key residues in place, four different stapling positions were designed into the Sld5 sequence by inspection of the Ctf4_{CTD}-Sld5 complex structure (PDB id: 4c95), including two sequences with conventional stapling at *i,i+7* and two unorthodox *i,i+6* and *i,i+8* staplings (Figure 3B). The diazido-peptides CF-A, CF-B, CF-C, CF-D (Figure 3B), where 'CF' represents N-terminal capping with 5(6)-carboxyfluorescein, were synthesised on Rink amide resin using automated solid-phase peptide synthesis. Copper-catalysed double-click macrocyclisations were subsequently performed with 1,3-diethynylbenzene (staple **1** in Figure 2A) to generate the corresponding bis-triazole stapled peptides CF-A1, CF-B1, CF-C1 and CF-D1.

Fluorescence anisotropy of stapled-peptide interactions with the Ctf4_{CTD}

The Sld5-based stapled peptides were first evaluated for their ability to bind Ctf4_{CTD} *in vitro* in a fluorescence anisotropy (FP) assay, using peptides that had been N-terminally labelled with carboxy-fluorescein (CF). The *i,i+6* stapled peptide A1 displayed a stronger binding affinity for Ctf4_{CTD} ($K_d = 0.84 \pm 0.19 \mu\text{M}$) compared to the wild-type peptide Sld5₁₋₁₉ ($K_d = 3.5 \pm 0.2 \mu\text{M}$), whereas the *i,i+7* stapled peptides B1 and C1 ($K_d = 18 \pm 1$ and $6.4 \pm 0.6 \mu\text{M}$ respectively) and the *i,i+8* peptide, D1, showed weaker binding to Ctf4 ($K_d = 15 \pm 1 \mu\text{M}$) (Figure 4A and Table 1).

As the Sld5 peptide A1, stapled at positions *i, i+6*, showed the strongest binding to Ctf4_{CTD}, it was further investigated using our divergent double-click stapling strategy to explore different staple scaffolds. The stapled peptide A2, which bears a linear aliphatic staple linkage (staple **2** in Figure 2A), was able to bind to Ctf4_{CTD} with a K_d of $0.32 \pm 0.02 \mu\text{M}$ (Figure 4B, Table 1 and Supplementary figure 1). Alternative aliphatic staples **3** and **4** (Figure 2A) were also investigated: the corresponding stapled peptides A3 and A4 bound to Ctf4 with comparable K_d values of $1.3 \mu\text{M}$, better than the wild-type peptide but not as tight as A2 (Figure 4B). However, the linkers in A3 and A4 provide attachment points for chemical derivatisation of the staple which could be exploited for instance to improve cell

permeabilization^{26,28}, while still retaining dissociation constants that are 2.7-fold stronger than the wild-type peptide.

FP analysis of A2 showed that its binding to Ctf4_{CTD} was one order of magnitude stronger than the wild-type peptide (Sld5₁₋₁₉). To confirm this improvement in the binding strength to Ctf4, we performed a competition experiment using CF-A2 peptide bound to Ctf4_{CTD}, and competed off the fluorescently-labelled peptide with unlabelled Sld5₁₋₁₉ or A2 peptides (Figure 4C). The competition experiment showed that A2 peptide is a better competitor for Ctf4 binding (apparent $K_d = 0.18 \mu\text{M}$) than the wild-type Sld5₁₋₁₉ peptide (apparent $K_d = 7.7 \mu\text{M}$).

Stapling of the Sld5 CIP increases its intrinsic α -helical nature

In the crystal structure of Ctf4_{CTD} bound to the Sld5 CIP, the peptide adopts a two-turn α -helical fold¹³ (Figure 3A). We set out to investigate whether the Sld5 CIP is intrinsically unfolded in solution, and whether stapling might promote α -helical structure in the A2 peptide that could explain its higher affinity for Ctf4. Circular dichroism (CD) analysis of Sld5₁₋₁₉ and A2 peptides indicated that they are largely unfolded in aqueous buffer (Figure 5), and that addition of tri-fluoroethanol (TFE) induced partial α -helix formation in both peptides, as expected (inset in Figure 5). In the absence of TFE however, we noticed a significant difference in α -helical content between the two peptides: whereas the wild-type Sld5 peptide is only 7% helical, the α -helix content of A2 is 21%, three times higher than wild-type. Conversely, the CD analysis of the diazido-peptide A, the modified peptide prior to double-click chemistry, suggests that its helical content is only 3%. Thus, it is reasonable to assume that the physical linkage between *i* and *i*+6 residues in the A2 peptide is responsible for its higher intrinsic α -helical content, which would account for its stronger binding to Ctf4.

Crystal structure of the stapled Sld5 CIP bound to Ctf4_{CTD}

To determine whether the mode of binding of A2 to Ctf4_{CTD} was as originally observed in the Ctf4_{CTD}-Sld5 CIP structure¹³ and to elucidate the conformation of the stapled Sld5 peptide bound to Ctf4_{CTD}, we determined the X-ray crystal structure of the Ctf4_{CTD}-A2 complex, by soaking the stapled peptide in crystals of Ctf4_{CTD} (Figure 6). The experiment showed that the A2 CIP binds Ctf4_{CTD} in an identical way to the wild-type Sld5 CIP, with no significant difference in peptide conformation. Interestingly, a reproducible improvement in diffraction properties of the Ctf4_{CTD} crystals was observed upon soaking of the A2 peptide, which provides further, indirect evidence that A2 has a stronger affinity for Ctf4_{CTD} than the wild-type Sld5 CIP. In the structure, the linear aliphatic bis-triazole linker is located on the opposite side of the A2 peptide relative to the Sld5 CIP - Ctf4_{CTD} interface, thus achieving the

conformation that had originally been planned. As such, the linker is fully exposed to solvent and must therefore attain its higher affinity by facilitating the adoption of the correct helical conformation for Ctf4_{CTD} binding via its stapling effect. The structure further shows that the triazole ring proximal to stapling position *i* packs against the salt link between Sld5 D7 and Ctf4 R904, providing further stabilisation of the Sld5 CIP - Ctf4_{CTD} interface.

The Sld5 CIP achieves a partial disruption of the GINS - Ctf4_{CTD} complex

We next investigated the ability of the wild-type Sld5 CIP and its stapled version A2 to interfere with the interaction between GINS and Ctf4_{CTD}. For this experiment, increasing amounts of peptide were incubated with reconstituted Ctf4_{CTD} - GINS complex and the samples were analysed by analytical gel filtration (Figure 7). The chromatographs were normalised and the relative ratios in peak height between GINS and the GINS - Ctf4_{CTD} complex were calculated as described in the methods (Figure 7A and 7B, inset). Addition of both wild-type Sld5 and stapled A2 peptide caused a partial disruption of the Ctf4_{CTD} - GINS complex in a concentration-dependent manner, as demonstrated by the reduction in peak size for the Ctf4_{CTD} - GINS complex and increase in the amount of free GINS. The disruptive effect of the Sld5 CIP peptides was noticeable but limited; the incomplete dissociation of the complex is in agreement with previous evidence indicating that the interaction surface between GINS and Ctf4_{CTD} extends beyond the Sld5-CIP binding site¹³. Nevertheless, at the highest concentration tested in the assay, the stapled peptide A2 was nearly twice more efficient than the wild-type Sld5 CIP.

The Sld5 CIP displaces a Ctf4 client from the replisome in yeast cell extracts

Our previous work showed that the CIP of Pol1, the catalytic subunit of yeast DNA polymerase α (Pol α), is required for Pol1 to associate with Ctf4 *in vitro*¹³. Moreover, mutations in the Pol1 CIP lead to displacement of Pol α from the replisome in yeast cells¹³. To explore whether it is possible to develop inhibitors of the interaction of Ctf4 with clients such as Pol1, we assayed the ability of the stapled or natural versions of the Sld5 CIP to disrupt the association of Pol α with the replisome in yeast cell extracts. After synchronising budding yeast cells in S-phase (Figure 8A), cell extracts were generated and incubated with or without Sld5-CIP or control peptides, before isolation of the replisome by immunoprecipitation of a tagged version of the Sld5 subunit of the CMG helicase (Figure 8B). Whereas none of the peptides disrupted the CMG helicase or its interactions with partners such as Csm3, the Sld5 CIP peptides specifically displaced Pol α from the replisome. Notably, stapled A2 version of the Sld5 CIP was more effective at lower concentrations than the wild-type Sld5 CIP (Figure 8B). In contrast to the complete disruption achieved for the association of Pol α with the replisome, the stapled version of the Sld5 CIP had a more modest effect on the association of Ctf4 with the CMG

helicase (Figure 8B). This is consistent with our past data showing that mutation of the Sld5 CIP does not displace Ctf4 from CMG¹³, presumably reflecting the more extensive nature of the interaction between Ctf4 and CMG. Correspondingly, the Sld5 CIP was only partially able to displace Ctf4 from the GINS component of the CMG helicase *in vitro* (Figure 5), though the stapled A2 peptide showed two-fold greater efficacy than the natural Sld5 CIP. Nevertheless, these data indicate that the stapled Sld5 CIP can efficiently inhibit the association of replisome-bound Ctf4 with client proteins such as Pol α .

Discussion

The experiments described here provide proof-of-principle evidence that it is possible to disrupt Ctf4's function in the replisome, by interfering with its ability to associate with CIP-box containing partner proteins such as Pol α . This has been achieved by the structure-based design of Ctf4-interacting peptides that include a staple linker for stabilisation and improved affinity. We have shown the design and biochemical validation of one such stapled peptide, A2, which contains the CIP sequence of the helicase subunit GINS Sld5, modified with a linear, aliphatic bis-triazole staple linking positions N4 and A10 of the wild-type Sld5 sequence. The stapled A2 peptide displays a higher affinity towards Ctf4_{CTD} than the wild-type sequence by about one order of magnitude, and is more effective at interfering with Ctf4 function, as determined by biochemical experiments with purified protein components and in yeast extracts.

The A2 peptide displayed limited take-up in yeast cells (F.V. and K.L., unpublished data with fluorescent versions of A2 generated by Y.W. and D.R.S.), which prevented us from assessing its ability to interfere with Ctf4 function *in vivo*. However, the method allows for a simple approach to garner cell permeability by modification of the staple^{26,28}. Future work will be required to fully explore the potential of stapled peptides to inhibit Ctf4 function in cells and tissues, perhaps by systematic derivatisation of the stapling group, which is facilitated by our two-component double-click stapling technique. Furthermore, our proof-of-concept work with stapled peptides will serve to inspire the development of small-molecule inhibitors with different pharmacological properties.

The role of Ctf4 as a hub in the replisome, coupling DNA synthesis to diverse molecular processes that pertain to chromosome replication and segregation, is likely to be conserved in diverse eukaryotic species. For example, the human orthologue of Ctf4 (also known as AND-1 or WDHD1) shares sequence conservation, domain structure, oligomerisation status and physiological roles with its yeast orthologue. It is therefore likely that human CTF4 will represent an attractive therapeutic target in the treatment of cancers carrying defects in CIN genes, and our work raises the prospect that it will be

possible to design inhibitors of the interaction of human CTF4 with its client proteins. Future efforts will be devoted to developing appropriate strategies, including the stapled-peptide approach demonstrated here, to target the biochemical function of CTF4 in human cells. As the type of peptide-protein interaction involving Ctf4 and its partner proteins is likely to represent a paradigm for the dynamic functional architecture of the replisome, such an approach might also be applicable to other instances of PPI between components of the human replisome.

Acknowledgments

This work was funded by a Wellcome Trust (reference 104641/Z/14/Z for investigator award to L.P., reference 102943/Z/13/Z for award to K.L.) and the Medical Research Council (core grant award MC_UU_12016/13 to KL). The Spring laboratory acknowledges support from the European Research Council under the European Union's Seventh Framework Programme (FP7/2007-2013)/ERC grant agreement no [279337/DOS]. In addition, the group research was supported by grants from the Engineering and Physical Sciences Research Council, Biotechnology and Biological Sciences Research Council, and Royal Society.

All data supporting this study are included in the paper and provided as Supporting Information accompanying this paper.

Accession numbers

The coordinates and structure factors for the crystal structure of Ctf4_{CTD} bound to the A2 peptide have been deposited in the Protein Data Bank under accession number 5NXQ.

Figure Legend

Figure 1. The drawing summarises our current understanding of Ctf4 function in the eukaryotic replisome, as a protein hub connecting replisome components such as the DNA helicase CMG and DNA polymerase α , as well as other factors such as the Dna2 helicase-nuclease and the Chl1 helicase. The oval inset shows a ribbon representation of the Ctf4_{CTD} trimer in purple, with bound CIPs as yellow cylinders.

Figure 2. A Double-click peptide stapling. The diazido-peptide is combined with different dialkynyl staples under Cu^I catalysis to obtain several bis-triazole stapled peptides. **B** Drawing illustrating the mechanism of targeting with stapled CIPs the interface of the Ctf4 trimer with its client proteins.

Figure 3. **A** Two views of the Ctf4_{CTD} - Sld5 CIP interface (PDB ID 4c95). **B** Sequence of the wild-type Sld5 CIP and of the A, B, C and D peptides. The stapling positions in each peptide are marked as **X** (all **X** = Orn(N₃)). The stapling positions of the A, B, C and D peptides are also shown mapped onto the structure of the Sld5 CIP bound to Ctf4_{CTD}, in four separate panels.

Figure 4. Fluorescence polarisation (FP) measurements of the affinity of stapled Sld5 CIPs towards Ctf4_{CTD}. **A** FP binding curves for stapled peptide A1 to B1, differing in stapling position. **B** FP binding curves for Sld5 CIPs stapled at *i*, *i+6*, in order to test different staple scaffolds. **C** FP competition experiment between wild-type Sld5 CIP and the stapled A2 peptide.

Figure 5. Circular dichroism (CD) analysis of wild-type Sld5 and stapled A2 CIPs. The CD spectra were recorded in the presence of 0, 15 and 30% tri-fluoroethanol (TFE).

Figure 6. X-ray crystal structure of Ctf4_{CTD} bound to the A2 peptide. **A** Close-up view of the A2 peptide structure, highlighting the position of the linear aliphatic bis-triazole linker. The stapling positions *i* and *i+6* are indicated by arrows. The final 2F_o - F_c electron density map contoured at 1σ for the refined crystallographic model is shown as a transparent surface, superimposed on the structure. **B** Superposition of the structure of Ctf4_{CTD} bound to the stapled A2 peptide and the wild-type Sld5 CIP (PDB id 4c95). Ctf4_{CTD} is shown as a light-brown ribbon, and the CIP peptides are drawn as sticks, in cyan (A2 peptide) and light sea green (Sld5 peptide).

Figure 7. Gel filtration assays measuring the ability of wild-type Sld5 and A2 CIPs to disrupt the Ctf4_{CTD} - GINS complex. The data was normalised relative to the total area under the combined peaks and expressed as the ratio of the GINS complex peak height to Ctf4_{CTD} - GINS complex peak height (insets). **A** Experiments performed in the presence of wild-type Sld5 CIP. **B** Experiments performed in the presence of the A2 peptide.

Figure 8. The Sld5 CIP displaces Pol α from the replisome in yeast cell extracts. **A** *TAP-SLD5* budding yeast cells (YSS47) were grown at 30 °C, arrested in G1 phase with mating pheromone, and then released into S phase for 20 minutes. DNA content was measured by flow cytometry. **B** The TAP-tagged Sld5 subunit of the CMG helicase was then isolated from cell extracts by immunoprecipitation in presence of the indicated stapled peptides or controls (the peptides were all dissolved in DMSO), and the indicated proteins were detected by immunoblotting with the corresponding antibodies.

Supplementary Figure Legend

Supplementary figure 1. Fluorescence polarisation (FP) measurements of the affinity of stapled Sld5 CIPs CF-A1 and CF-A2 towards Ctf4_{CTD}.

References

1. Cheung-Ong, K., Giaever, G. & Nislow, C. DNA-Damaging Agents in Cancer Chemotherapy: Serendipity and Chemical Biology. *Chemistry & Biology* **20**, 648–659 (2013).
2. Lord, C. J. & Ashworth, A. The DNA damage response and cancer therapy. *Nature* **481**, 287–294 (2012).
3. O'Connor, M. J. Targeting the DNA Damage Response in Cancer. *Mol. Cell* **60**, 547–560 (2015).
4. Plunkett, W., W, P., P, H., Huang, P. Gandhi, V. Metabolism and action of fludarabine phosphate. *Semin Oncol* **17**, 3–17 (1990).
5. Lukenbill, J. & Kalaycio, M. Fludarabine: A review of the clear benefits and potential harms. **37**, 986–994 (2013).
6. Liu, Y.-Q. *et al.* Perspectives on biologically active camptothecin derivatives. *Med Res Rev* **35**, 753–789 (2015).
7. Hande, K. R. Etoposide: four decades of development of a topoisomerase II inhibitor. *European Journal of Cancer* **34**, 1514–1521 (1998).
8. van Pel, D. M., Stirling, P. C., Minaker, S. W., Sipahimalani, P. & Hieter, P. *Saccharomyces cerevisiae* genetics predicts candidate therapeutic genetic interactions at the mammalian replication fork. *G3 (Bethesda, Md.)* **3**, 273–282 (2013).
9. Yuen, K. W. Y. *et al.* Systematic genome instability screens in yeast and their potential relevance to cancer. *Proc. Natl. Acad. Sci. U.S.A.* **104**, 3925–3930 (2007).
10. Kouprina, N. *et al.* CTF4 (CHL15) mutants exhibit defective DNA metabolism in the yeast *Saccharomyces cerevisiae*. *Mol. Cell. Biol.* **12**, 5736–5747 (1992).
11. Miles, J. & Formosa, T. Evidence that POB1, a *Saccharomyces cerevisiae* protein that binds to DNA polymerase alpha, acts in DNA metabolism in vivo. *Mol. Cell. Biol.* **12**, 5724–5735 (1992).
12. van Pel, D. M. *et al.* An evolutionarily conserved synthetic lethal interaction network identifies FEN1 as a broad-spectrum target for anticancer therapeutic development. *PLoS Genet.* **9**, e1003254 (2013).
13. Simon, A. C. *et al.* A Ctf4 trimer couples the CMG helicase to DNA polymerase alpha in the eukaryotic replisome. *Nature* **510**, 293–297 (2014).
14. Villa, F. *et al.* Ctf4 Is a Hub in the Eukaryotic Replisome that Links Multiple CIP-Box Proteins to the CMG Helicase. *Mol. Cell* **63**, 385–396 (2016).
15. Davey, N. E. *et al.* Attributes of short linear motifs. *Molecular bioSystems* **8**, 268–281 (2012).
16. Tompa, P., Davey, N. E., Gibson, T. J. & Babu, M. M. A million peptide motifs for the molecular biologist. *Mol. Cell* **55**, 161–169 (2014).
17. Pellegrini, L. & Costa, A. New Insights into the Mechanism of DNA Duplication by the Eukaryotic Replisome. *Trends Biochem. Sci.* **41**, 859–871 (2016).
18. Higuero, A. P., Jubb, H. & Blundell, T. L. Protein–protein interactions as druggable targets: recent technological advances. *Current Opinion in Pharmacology* **13**, 791–796 (2013).
19. Arkin, M. R., Tang, Y. & Wells, J. A. Small-molecule inhibitors of protein-protein interactions: progressing toward the reality. *Chemistry & Biology* **21**, 1102–1114 (2014).
20. Laraia, L., McKenzie, G., Spring, D. R., Venkitaraman, A. R. & Huggins, D. J. Overcoming

- Chemical, Biological, and Computational Challenges in the Development of Inhibitors Targeting Protein-Protein Interactions. *Chemistry & Biology* **22**, 689–703 (2015).
21. Walensky, L. D. & Bird, G. H. Hydrocarbon-stapled peptides: principles, practice, and progress. *J. Med. Chem.* **57**, 6275–6288 (2014).
 22. Rezaei Araghi, R. & Keating, A. E. Designing helical peptide inhibitors of protein–protein interactions. *Curr. Opin. Struct. Biol.* **39**, 27–38 (2016).
 23. Verdine, G. L. & Hilinski, G. J. Stapled peptides for intracellular drug targets. *Meth. Enzymol.* **503**, 3–33 (2012).
 24. Lau, Y. H., de Andrade, P., Wu, Y. & Spring, D. R. Peptide stapling techniques based on different macrocyclisation chemistries. *Chemical Society Reviews* **44**, 91–102 (2015).
 25. Bird, G. H. *et al.* Biophysical determinants for cellular uptake of hydrocarbon-stapled peptide helices. *Nat Chem Biol* **12**, 845–852 (2016).
 26. Lau, Y. H. *et al.* Functionalised staple linkages for modulating the cellular activity of stapled peptides. *Chem. Sci.* **5**, 1804–1809 (2014).
 27. Lau, Y. H. *et al.* Double Strain-Promoted Macrocyclization for the Rapid Selection of Cell-Active Stapled Peptides. *Angewandte Chemie International Edition* **54**, 15410–15413 (2015).
 28. Xu, W. *et al.* Macrocyclized Extended Peptides: Inhibiting the Substrate-Recognition Domain of Tankyrase. *J. Am. Chem. Soc.* **139**, 2245–2256 (2017).
 29. Lau, Y. H., Wu, Y., de Andrade, P., Galloway, W. R. J. D. & Spring, D. R. A two-component ‘double-click’ approach to peptide stapling. *Nat. Protocols* **10**, 585–594 (2015).
 30. Wiedmann, M. M. *et al.* Development of Cell-Permeable, Non-Helical Constrained Peptides to Target a Key Protein-Protein Interaction in Ovarian Cancer. *Angewandte Chemie International Edition* **56**, 524–529 (2017).

Table 1. Binding affinities of Sld5 peptides for Ctf4_{CTD}

Peptide	K_d (μM)
CF-Sld5₁₋₁₉	3.5 ± 0.2
CF-A1	0.75 ± 0.03
CF-B1	18 ± 1
CF-C1	6.4 ± 0.6
CF-D1	15 ± 1
CF-A2	0.37 ± 0.01
CF-A3	1.3 ± 0.2
CF-A4	1.3 ± 0.1

Table 2. Data collection and refinement statistics

Wavelength	
Resolution range	49.21 - 2.413 (2.499 - 2.413)
Space group	P 2 21 21
Unit cell	88.679 100.287 219.749 90 90 90
Total reflections	1003177 (90575)
Unique reflections	76177 (7499)
Multiplicity	13.2 (12.1)
Completeness (%)	99.96 (99.83)
Mean I/sigma(I)	14.80 (1.03)
Wilson B-factor	58.96
R-merge	0.1424 (2.453)
R-meas	0.1482 (2.563)
R-pim	0.04074 (0.7354)
CC1/2	0.999 (0.329)
CC*	1 (0.703)
Reflections used in refinement	76170 (7499)
Reflections used for R-free	3805 (365)
R-work	0.1804 (0.3461)
R-free	0.2108 (0.3733)
CC(work)	0.969 (0.644)
CC(free)	0.968 (0.565)
Number of non-hydrogen atoms	9971
macromolecules	9552
ligands	60
solvent	359
Protein residues	1181
RMS(bonds)	0.003
RMS(angles)	0.59
Ramachandran favored (%)	96.26
Ramachandran allowed (%)	3.30
Ramachandran outliers (%)	0.43
Rotamer outliers (%)	0.19
Clashscore	2.11
Average B-factor	67.98
macromolecules	68.08
ligands	97.55
solvent	60.43

Statistics for the highest-resolution shell are shown in parentheses.

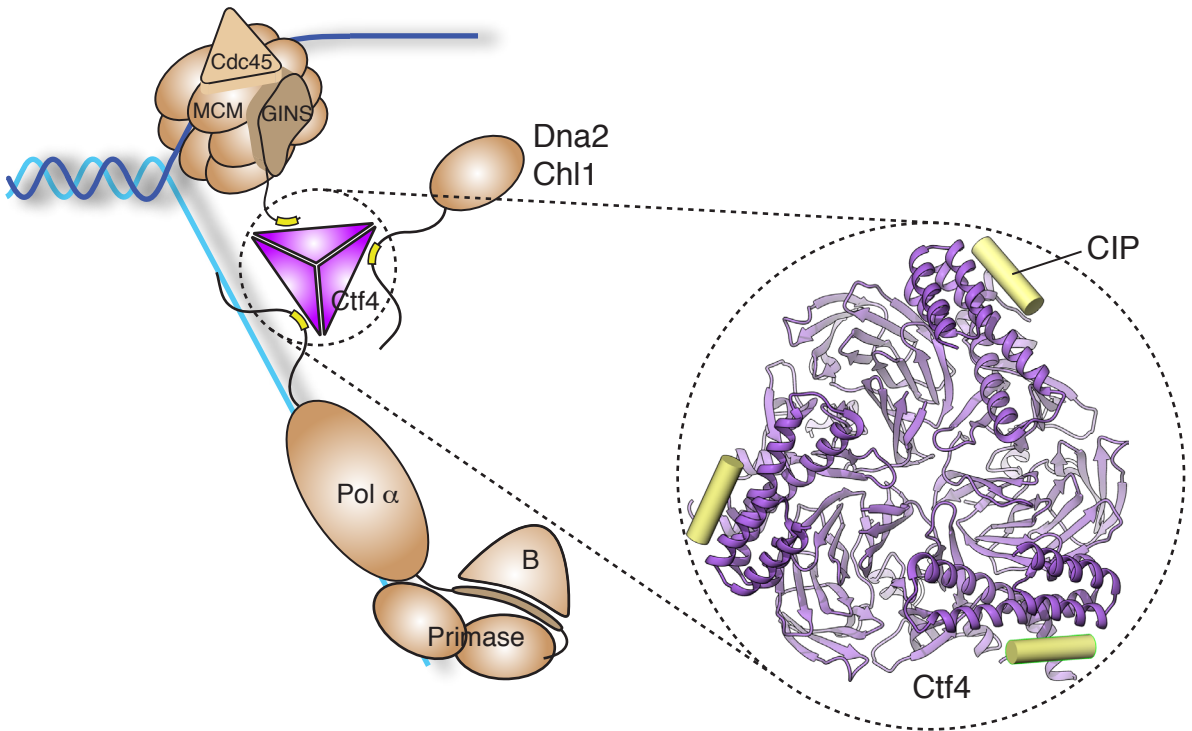


Figure 1

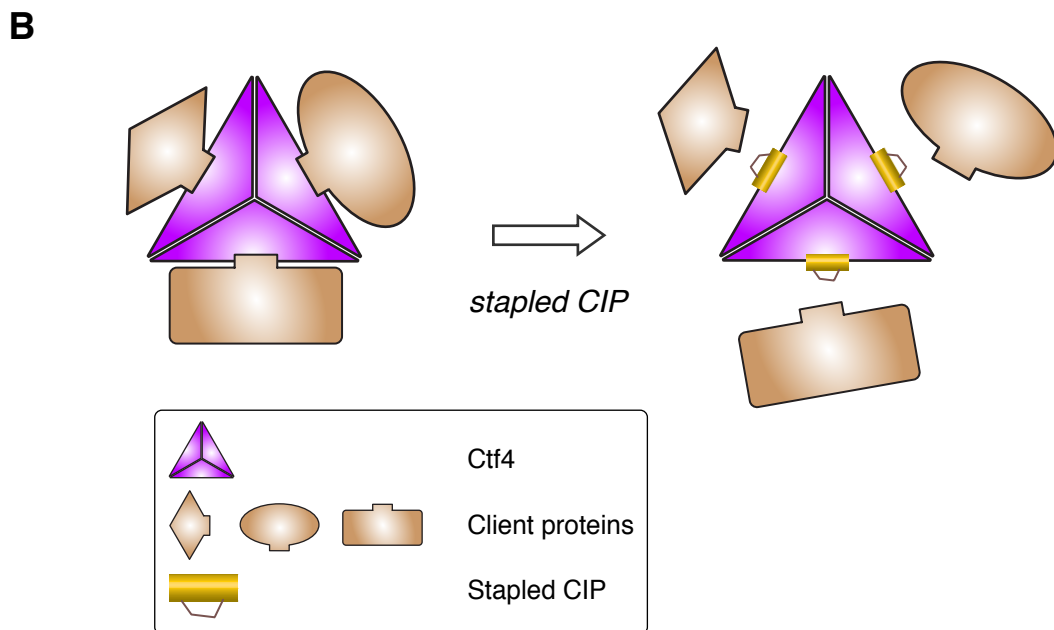
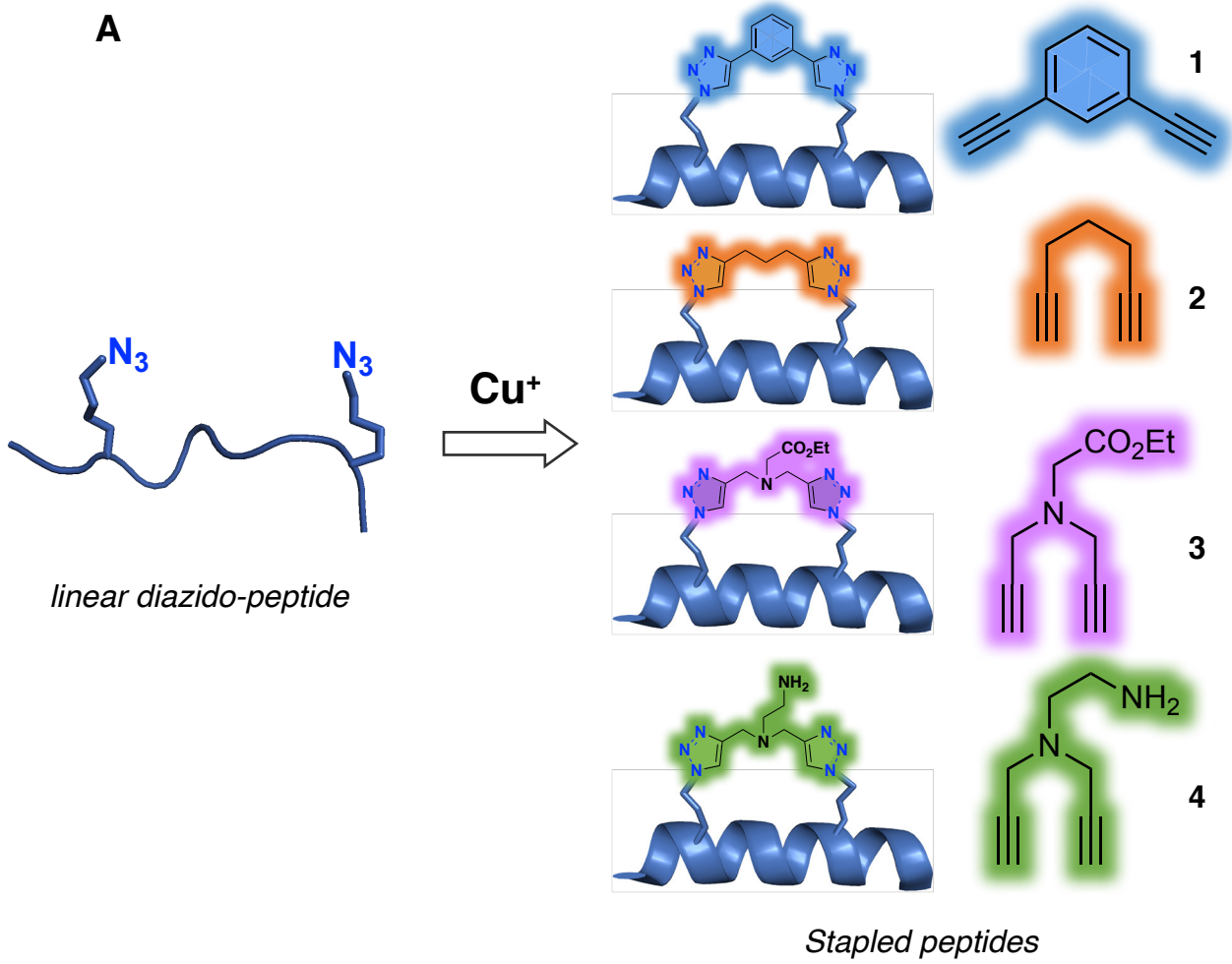


Figure 2

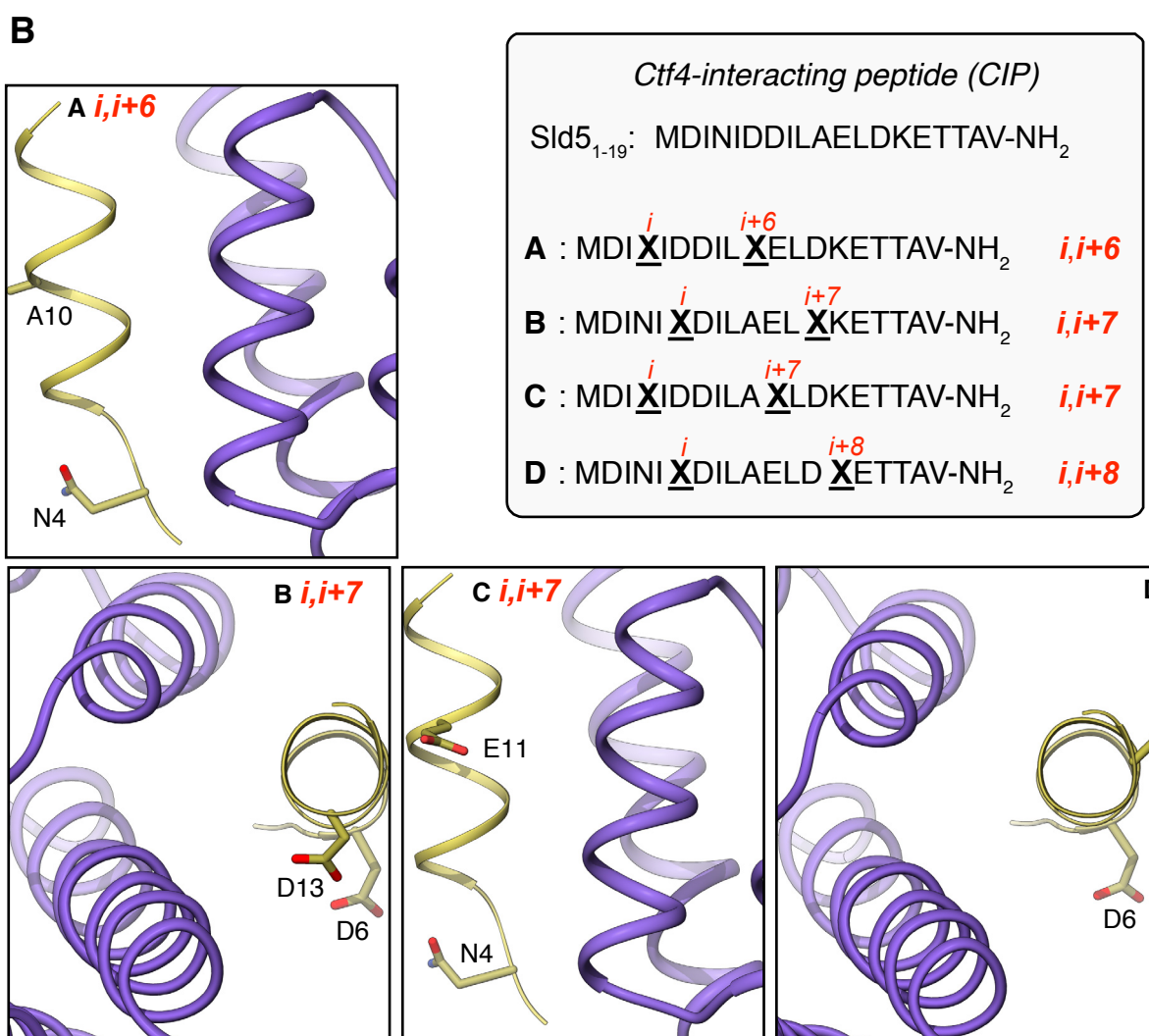
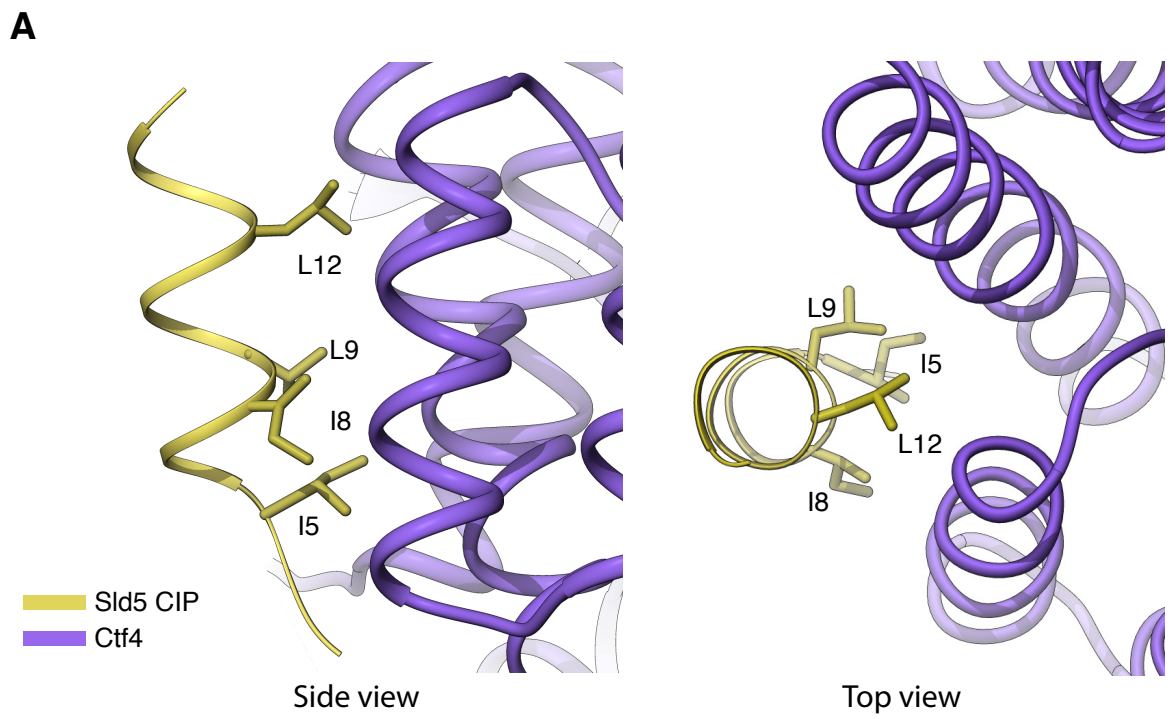


Figure 3

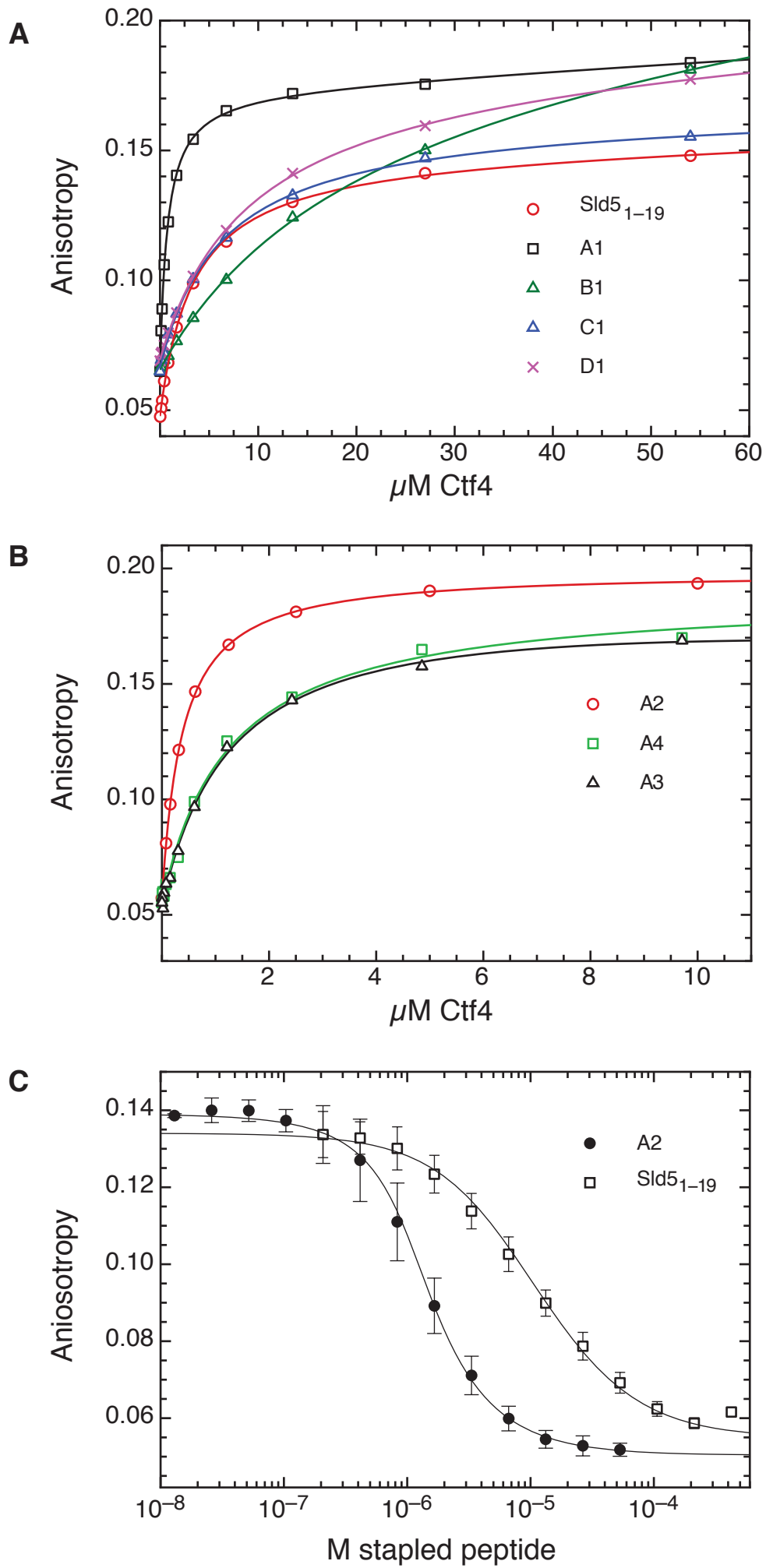
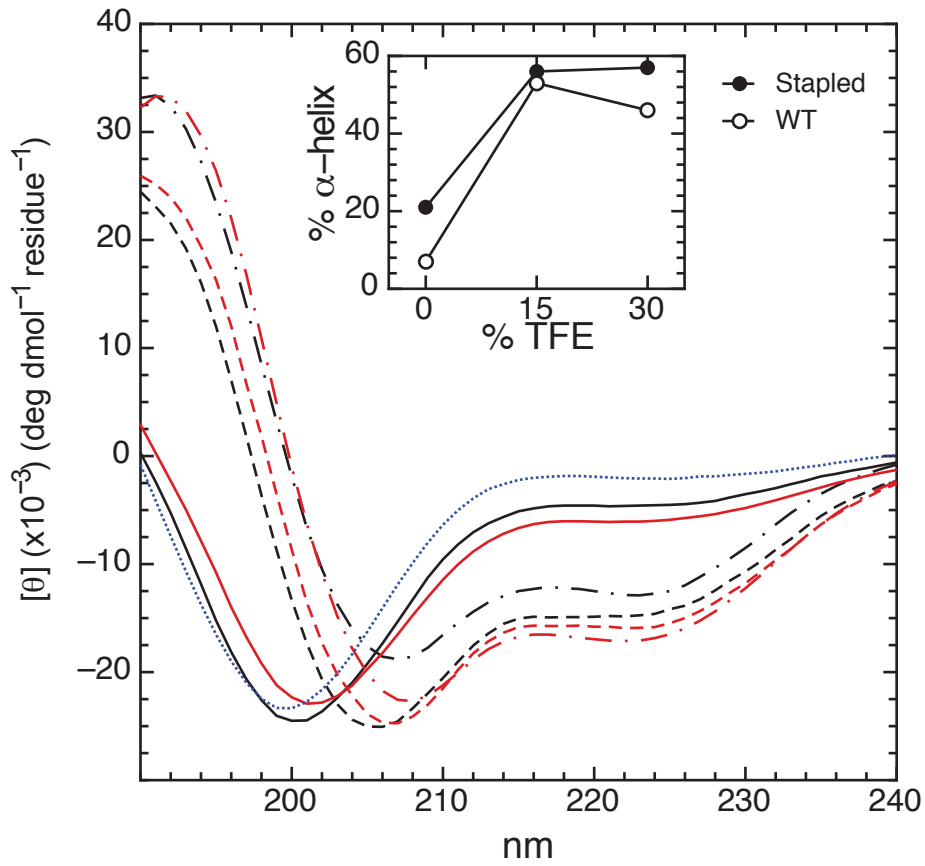


Figure 4



- Sld5₁₋₁₉
- - - Sld5₁₋₁₉ + 15% TFE
- · - Sld5₁₋₁₉ + 30% TFE
- A2
- - - A2 + 15% TFE
- · - A2 + 30% TFE
- unstapled A2

Figure 5

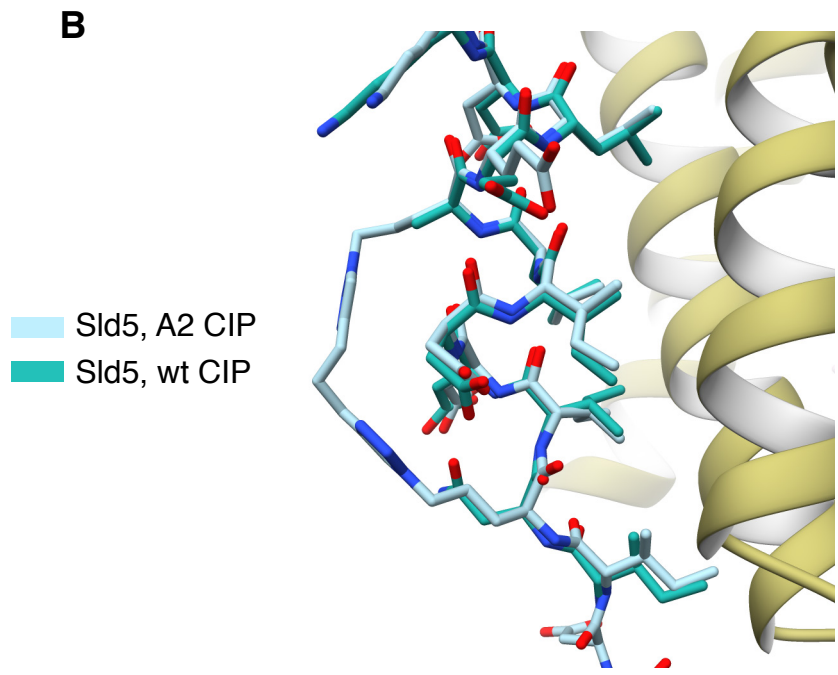
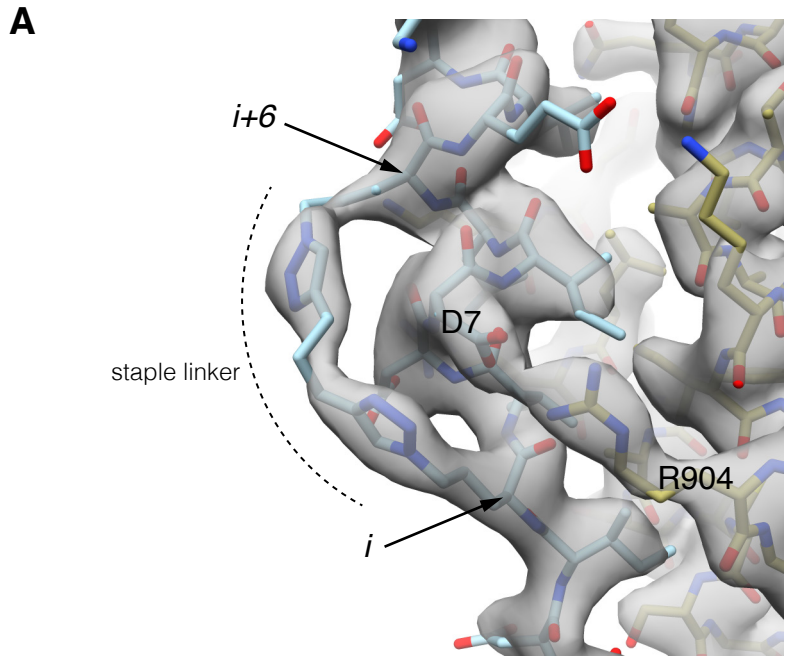


Figure 6

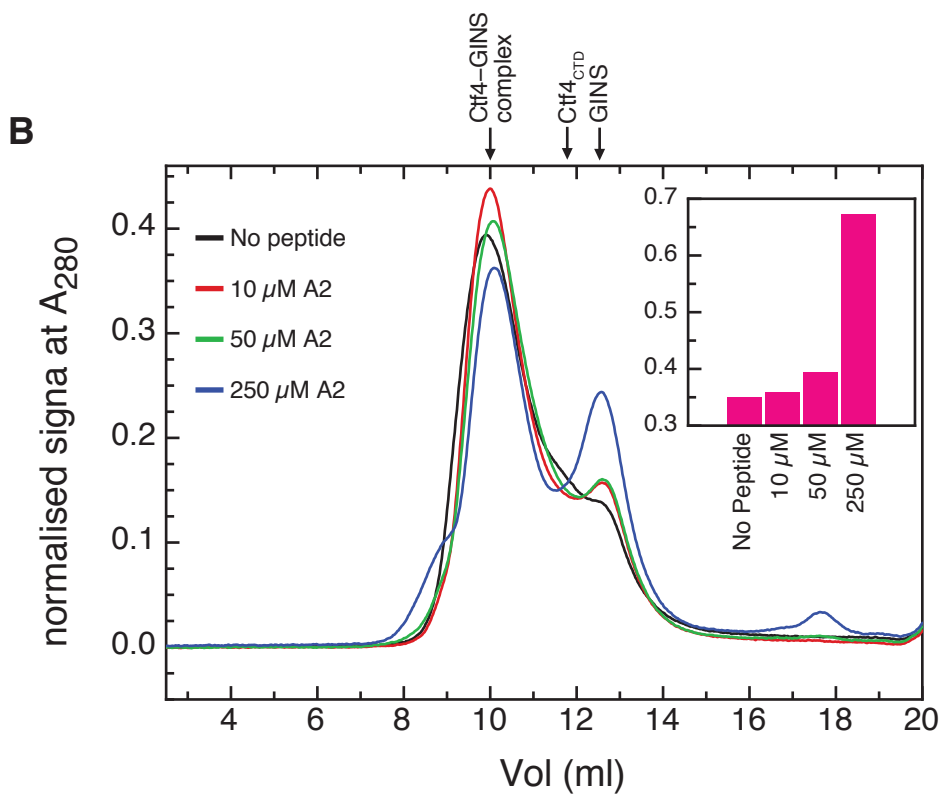
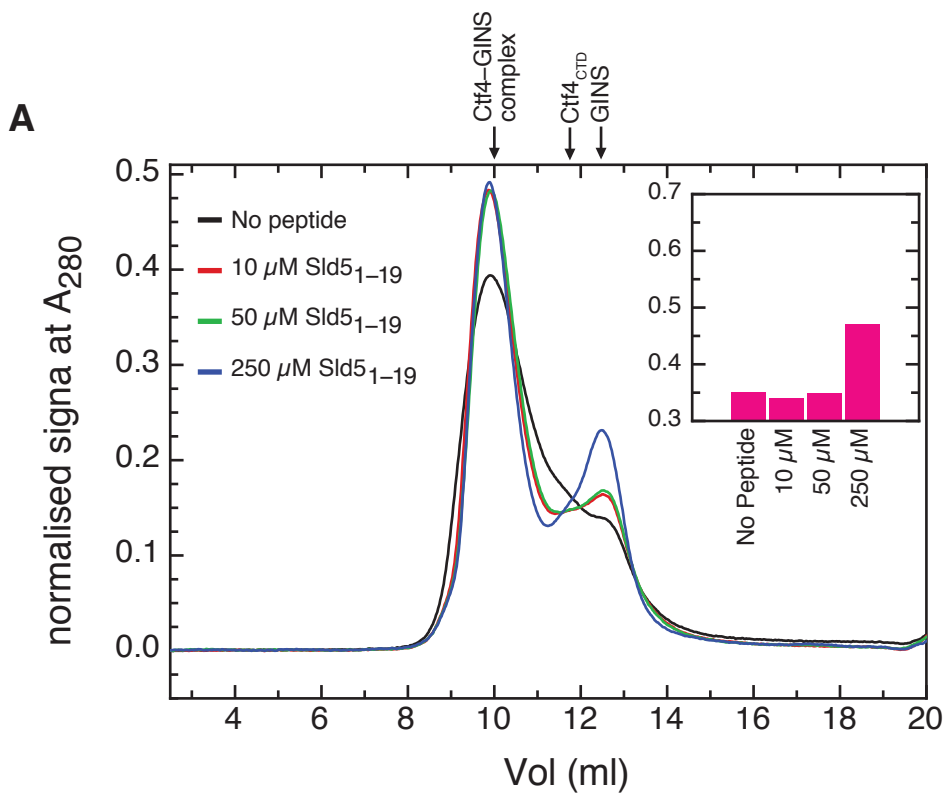
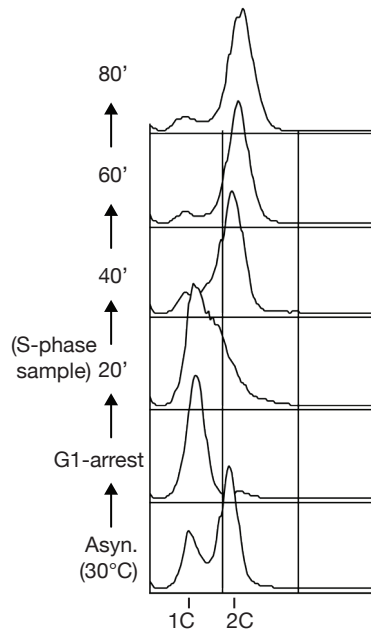
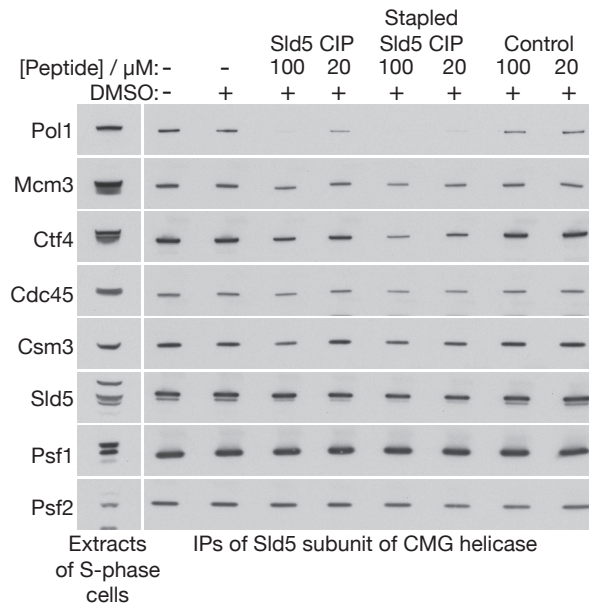


Figure 7

A**B****Figure 8**